Biaxial Deformation of a Polymer Network Measured via Deuteron Quadrupolar Interactions

P. T. Callaghan[†] and E. T. Samulski[‡]

MacDiarmid Institute for Advanced Materials and Nanotechnology, School of Chemical and Physical Sciences, Victoria University of Wellington, Wellington, New Zealand, and Department of Chemistry, University of North Carolina at Chapel Hill, Chapel Hill, North Carolina 27599-3290

Received July 23, 2002

ABSTRACT: Deuterium quadrupolar interactions have been used to measure chain ordering for poly(dimethylsiloxane) elastomers under planar biaxial extension. The NMR spectral splittings obtained from two different deuterium-labeled probe molecules diffusing within the network were measured as a function of extension ratio λ and the orientation of the principal axis of deformation with respect to the magnetic field. Theoretical predictions based on a phantom Gaussian chain model are compared with the data and good agreement is found. The implications of axial asymmetry at various levels of the probe molecule motional hierarchy are discussed. For rapidly diffusing probe molecules, only the highest level in the hierarchy influences the observed quadrupole interaction symmetry, and the true distribution of chain segment directors is measured.

1. Introduction

The use of deuterium quadrupolar interactions to study uniaxial deformation in polymer networks is well-established.[1−11] In particular, the quadrupole splitting, obtained from a small deuterated probe molecule diffusing within the network, is known to be sensitive to the network strain, with the splitting dependence on the deformation ratio $\lambda = L/L_0$ given by[1,13] $\Delta\omega \sim (\lambda^2 - \lambda^{-1})$.

A typical probe molecule might be a deuterated monomer or oligomer of the same chemical composition as the polymer network, or some other small deuterated molecule which is soluble within the network. As this molecule diffuses within the network, it occasionally collides with the polymer segments and suffers anisotropic steric hindrance, thus being slightly constrained in available orientation. This steric sensitivity to the polymer segment orientation is sometimes termed a "pseudonematic interaction".[1] It enables the probe molecule to "inherit" the orientational order of the host network, albeit significantly reduced by a numerical factor whose precise magnitude depends on the subtle details of interaction averaging.

All NMR experiments on deformed elastomers reported to date concern uniaxial deformations in which the network is either stretched or compressed along a single axis while being allowed to freely deform in the remaining two orthogonal directions.[1−10] The cylindrical symmetry inherent in such a deformation leads to a simple angular dependence of the quadrupole splitting as the principal axis is inclined away from the magnetic field, namely that of the second Legendre polynomial, $P_2(\cos\alpha)$. In such systems, the degree of deformation, λ, determines the absolute magnitude of the splitting, but the angular dependence is independent of λ. In this article, we report on experiments carried out in networks which are biaxially deformed. In this case, the angular dependence of the deuterium splitting so measured is strongly dependent on λ. We derive expressions for this angular dependence and compare the results with experiments.

There are specific reasons for wishing to carry out such a test. First, we note that uniaxial deformations lead to a quadrupole splitting for which the strain dependence and angular dependence are entirely separable, the latter being in no way connected with the details of the microscopic model used. This is not so for biaxiality, and thus a measurement of angular dependence provides a test of model assumptions, in this work those inherent in the phantom Gaussian chain model. Second, we note that there has been recent interest in the use of ordered environments for NMR studies of protein structure.[14−16] For example, generation of a small degree of orientational order in proteins, by immersing them in the nematic environment provided by lyotropic micellar liquid crystals, has proven exceptionally powerful.[14,15] While a uniaxial liquid crystal environment can give information about the average polar angles with respect to the B_0 field made by internuclear vectors within the protein, nothing is learned about the azimuth angles. For that one needs an environment where the proteins were azimuthally oriented. A biaxial liquid crystal environment or possibly a strained biaxial network environment could prove useful in this regard.[16,17]

A network consists of distinct random coil polymer chains bounded by cross-links, as shown in Figure 1. The quiescent network is considered to comprise Gaussian chains tethered by cross-links which represent junction points. Each chain is defined by an end-to-end vector **R** spanning those cross-linked end points. While the polymer segments in that chain may fluctuate in orientation, their mean direction will be given by the direction of **R** while their mean orientational order will depend on the magnitude of **R**. In other words, the degree to which local polymer segments are able to sample the configurational space of possible orientations will depend on the degree to which the chains are stretched. A probe molecule in the vicinity of a given chain will inherit alignment according to these properties of **R**. To understand this process, it is necessary to

[†] Victoria University of Wellington.
[‡] University of North Carolina at Chapel Hill.

10.1021/ma021174z CCC: $25.00
Published on Web 01/04/2003

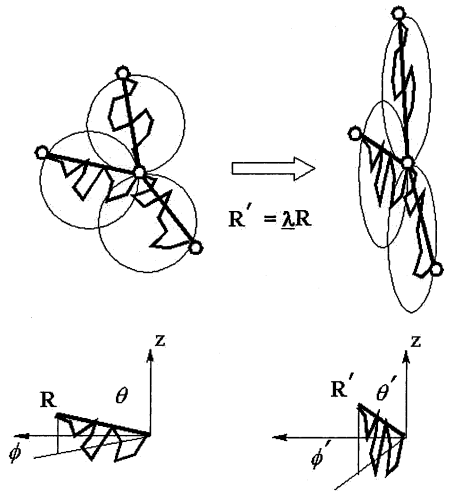

Figure 1. Schematic illustration of network chains connecting a constellation of junction points. The spheroidal volume pervaded by Gaussian chains in the quiescent network (left) is perturbed when the network is deformed (right). Defined relative to the principal axis of the strain tensor *l* (*z* axis), end-to-end vectors (bold lines) of network chains prior to the deformation, $\mathbf{R}(\theta,\phi)$, are transformed to new lengths and orientations $\mathbf{R}'(\theta',\phi')$ by the applied strain.

invoke the concept of motional averaging. As the probe molecule diffuses within the network, the local quadrupole interactions will fluctuate as the molecule first encounters different polymer segments whose orientations fluctuate about **R** and then, subsequently, different network chains with different **R** vectors. There is thus a motional hierarchy. However, the probe molecules used in our work experience an average over the entire hierarchy since the characteristic time associated with the local quadrupole interaction strength (typically milliseconds) is on the order of the time taken to diffuse between a complete representative ensemble of network chains (typically micrometers).

2. Theory

2.1. Quadrupolar Interactions for Probe Molecules in a Network. The quadrupole interaction of the spin-1 deuteron is measured in the presence of the much larger magnetic Zeeman interaction and so is observed as a first-order perturbation projected along the zeroth order quantisation axis of the magnetic field.[18,19] Most often, the quadrupole interaction arises from the axially symmetric electric field gradient associated with the molecular orbital along a C−D bond of the labeled molecule. Consider first the case of a probe molecule deuteron whose C−D bond experiences an instantaneous orientation with respect to the magnetic field defined by the polar angle $\theta(t)$. Then the quadrupole interaction may be written[16]

$$H_Q(t) = AP_2(\cos\theta(t))[3I_{1z}I_{2z} - I_1I_2] \qquad (1)$$

where P_2 is the second Legendre polynomial and the interaction strength parameter, A, is $3eV_{zz}Q/4h$—where V_{zz} is the electric field gradient (efg) along the principal axis and Q is the nuclear quadrupole moment. The bilinear nature of the interaction with respect to the spin operators leads to a two-line spectrum whose splitting is determined by H_Q.

Because the efg principal axis is associated with an interatomic bond direction within the molecule, $\theta(t)$ fluctuates due to molecular motion. Provided that motion is fast compared with the interaction strength, A, the fluctuating Hamiltonian is motionally averaged to its mean. Consider the case in which the bond orientation (θ,φ) with respect to B_0 can be decomposed into $(\theta_\alpha,\varphi_\alpha)$ with respect to an axis inclined at polar angle α with respect to B_0, where $(\theta_\alpha,\varphi_\alpha)$ fluctuates rapidly and α very slowly compared with the motional narrowing condition. Then the spherical harmonic addition theorem may be used to factorize as follows[20]

$$\overline{P_2(\cos\theta(t))} = \overline{P_2(\cos\theta_\alpha(t))_{fast}}\, P_2(\cos\alpha) \qquad (2)$$

In effect the spin system experiences an interaction with director along α and with a strength scaled down by the order parameter $\overline{P_2(\cos\theta_\alpha(t))_{fast}}$.

Consider the case of a Gaussian random coil chain of mean squared chain length R_0^2. Suppose that chain is fixed at its end points, with end-to-end vector **R**, inclined at α to the magnetic field direction. We will assume that a deuteron sited within a diffusing probe molecule samples that chain. Then the term $\overline{P_2(\cos\theta_\alpha(t))_{fast}}$ in eq 2 allows for the fluctuations both of the polymer segment orientations about the mean end-to-end vector as well as the further reduction due to the indirect nature of the probe molecule steric interactions. Sotta and Deloche[7] have shown that this reduction term arising from segmental reorientation contributes a factor proportional to $\mathbf{R}\cdot\mathbf{R}/R_0^2$. The term $\cos\alpha$ in eq 2 is given by $\mathbf{R}\cdot\boldsymbol{k}/R$ where **k** is the unit vector along B_0 which defines the laboratory frame *z* axis and $R = |\mathbf{R}|$. In summary, the probe molecule will exhibit a deuteron spectrum split by $\Delta\omega$ where

$$\Delta\omega = \omega_0\left(\frac{R}{R_0}\right)^2 P_2(\cos\alpha) \qquad (3)$$

and ω_0 is a fixed value which is determined by the details of the probe molecule and its concentration in the network.

Next we consider an undeformed network of chains for which the distribution of chain vectors is isotropic and assume that the probe molecules sample a full representative ensemble of network chains. Finding the mean splitting involves taking an ensemble average of the term $\Delta\omega$ in eq 3. This involves integrating over the Gaussian probability for the original R and the uniform (isotropic) distribution of the original direction cosine, $\cos\alpha$, i.e.

$$\Delta\omega = \omega_0 R_0^{-2}\left\langle R^2\frac{1}{2}(3\cos\alpha^2 - 1)\right\rangle_{R,\cos\alpha} \qquad (4)$$

For an unstrained network, the averages over R and α are separable. By definition $\langle R^2\rangle_R = R_0^2$ and for an isotropic distribution $\langle {}^1/_2(3\cos\alpha^2 - 1)\rangle_{\cos\alpha} = 0$. Thus, no splitting is observed for the unstrained network even though locally the direction of the constraint (**R**) is fixed in space. This is reminiscent of fast probe diffusion in liquid crystals having a cubic supramolecular structure.[21]

2.2. The Consequences of Deformation. An affine deformation of the network causes all vectors, **R**, within the material to be transformed according to[22]

$$\mathbf{R}' = \boldsymbol{\lambda}\mathbf{R} \qquad (5)$$

where $\boldsymbol{\lambda}$ is the deformation tensor. The effect on an individual Gaussian chain is shown in Figure 1. To

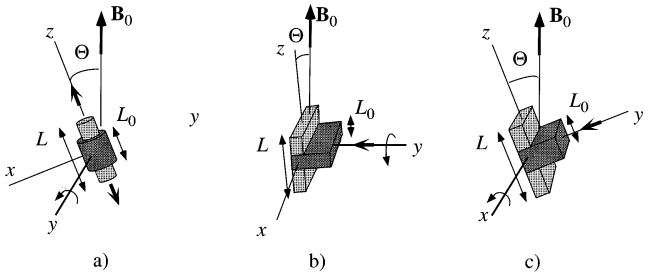

Figure 2. Relative orientation of the magnetic field, and the principal axis of the deformation (the sample z axis) for uniaxial (a) and biaxial (b and c) deformations illustrated for strains, $\lambda = L/L_0$. The arrows in the diagrams indicate uniaxial extension and biaxial compression, respectively. In part b, the sample is reoriented in the plane $x-z$ and in part c in the plane $y-z$.

describe what happens to the deuterium NMR spectrum, we may define the deformation tensor within the B_0 frame and label it $\boldsymbol{\lambda}_{B_0}$ accordingly. The length of the end-to-end vector, R', its direction cosine, cos α', with respect to the magnetic field direction, z, and its azimuth, ϕ', will all be perturbed from their initial values. These changes are simply related to the properties of the unperturbed vector, **R**, via the deformation tensor, $\boldsymbol{\lambda}_{B_0}$. Under deformation eq 3 is reevaluated, as

$$\begin{aligned}\Delta\omega &= \omega_0\left\langle\left(\frac{R'}{R_0}\right)^2 P_2(\cos\alpha')\right\rangle_{R',\cos\alpha'} \\ &= \omega_0 {R_0}^{-2}\left\langle R'^2 \frac{1}{2}(3\cos^2\alpha' - 1)\right\rangle_{R',\cos\alpha'} \\ &= \omega_0 {R_0}^{-2}\left\langle R'^2 \frac{1}{2}(3\cos^2\alpha' - 1)\right\rangle_{R,\cos\alpha,\phi} \qquad (6)\end{aligned}$$

where the ensemble averages are again taken over the Gaussian probability for the original R^2, and the uniform (isotropic) distribution of the original polar direction cosine, cos α, and azimuth, ϕ. Note that both R'^2 and $\cos^2\alpha'$ depend on the initial squared length R^2 and the initial polar and azimuthal orientations of the chain. Note that eq 6 is equivalent to the expression $\omega_0 {R_0}^{-2}$ $^1/_2\langle 2R_z'^2 - R_x'^2 - R_y'^2\rangle_{R,\cos\alpha,\phi}$.

2.3. Uniaxial Deformation. For a volume-conserving uniaxial deformation with elongation ratio $\lambda = L/L_0$, the deformation tensor, in the deformation (principal axis) frame, is[22]

$$\boldsymbol{\lambda} = \begin{bmatrix} \lambda^{-1/2} & 0 & 0 \\ 0 & \lambda^{-1/2} & 0 \\ 0 & 0 & \lambda \end{bmatrix} \qquad (7)$$

Such a deformation may be performed by stretching the network along an axis (as shown in Figure 2a) and allowing free contraction in the remaining directions ($\lambda > 1$), or by squeezing and allowing free expansion ($\lambda < 1$). The stretch or squeeze direction defines the principal axis. Suppose that the principal axis of the deformation is inclined at Θ to the magnetic field. We will describe the deformation in the frame of that field, with the rotation arbitrarily, and without loss of generality, taken as being about the y axis so that the magnetic field direction lies in the $x-z$ plane of the principal axis frame of the deformation. To do this we must apply the rotation matrix for a rotation about y, i.e.

$$R_y(\theta) = \begin{bmatrix} \cos\Theta & 0 & \sin\Theta \\ 0 & 1 & 0 \\ -\sin\Theta & 0 & \cos\Theta \end{bmatrix} \qquad (8)$$

For convenience we will use $c = \cos\Theta$, $s = \sin\Theta$. Thus, the transformed λ is

$$\boldsymbol{\lambda}_{B_0} = \begin{bmatrix} c^2\lambda^{-1/2} + s^2\lambda & 0 & cs(\lambda - \lambda^{-1/2}) \\ 0 & \lambda^{-1/2} & 0 \\ cs(\lambda - \lambda^{-1/2}) & 0 & s^2\lambda^{-1/2} + c^2\lambda \end{bmatrix} \qquad (9)$$

2.4. Planar Biaxial Deformation. A planar biaxial deformation may be achieved by squeezing the network in one direction, allowing free expansion in one orthogonal direction and constraining the dimensions of the sample in the second orthogonal direction. An example of such a deformation is shown in Figure 2, parts b and c. The deformation tensor, in the principal axis frame, is

$$\boldsymbol{\lambda} = \begin{bmatrix} 1 & 0 & 0 \\ 0 & \lambda^{-1} & 0 \\ 0 & 0 & \lambda \end{bmatrix} \qquad (10)$$

By convention we shall take $\lambda > 1$ and define the z axis in the deformation frame as the "stretch" axis. Note that for this deformation, we may identify either of the "neutral", "squeeze", or "stretch" directions as the principal axis. Again, we consider the possibility that the principal axis frame is inclined at Θ to the magnetic field. Clearly there are three ways in which the azimuthal orientation of the principal axis may be inclined, namely by rotating the sample so that the magnetic field lies in either of the $x-z$, $y-z$, or $x-y$ planes.

For the moment, and by way of example, we will define the rotation as being about the y axis so that the magnetic field direction lies in the $x-z$ plane of the principal axis frame of the deformation. This geometry is illustrated in Figure 2b. Note that the x axis of the deformation frame is the neutral direction so that the field varies from being along the neutral axis to the stretch axis. Thus, the transformed $\boldsymbol{\lambda}$ is

$$\boldsymbol{\lambda}_{B_0} = \begin{bmatrix} c^2 + s^2\lambda & 0 & cs(\lambda - 1) \\ 0 & \lambda^{-1} & 0 \\ cs(\lambda - 1) & 0 & s^2 + c^2\lambda \end{bmatrix} \qquad (11)$$

2.5. Mean Spectrum for Uniaxial Deformation. We wish to evaluate eq 6 under the deformation shown in eq 9. Now we may use the fact that

$$\begin{aligned} R_x' &= (c^2\lambda^{-1/2} + s^2\lambda)R_x + cs(\lambda - \lambda^{-1/2})R_z \\ R_y' &= \lambda^{-1/2}R_y \\ R_z' &= cs(\lambda - \lambda^{-1/2})R_x + (s^2\lambda^{-1/2} + c^2\lambda)R_z \end{aligned} \qquad (12)$$

where

$$R_x = R \sin\alpha \cos\phi$$
$$R_y = R \sin\alpha \sin\phi$$
$$R_z = R \cos\alpha \quad (13)$$

Thus

$$R'^2 = R^2[(c^2\lambda^{-1/2} + s^2\lambda)^2 \sin^2\alpha \cos^2\phi + 2(c^2\lambda^{-1/2} + s^2\lambda)cs(\lambda - \lambda^{-1/2}) \sin\alpha \cos\alpha \cos\phi + c^2s^2(\lambda - \lambda^{-1/2})^2\cos^2\alpha + \lambda^{-1}\sin^2\alpha \sin^2\phi + c^2s^2(\lambda - \lambda^{-1/2})^2 \sin^2\alpha \cos^2\phi + 2(s^2\lambda^{-1/2} + c^2\lambda)cs(\lambda - \lambda^{-1/2}) \sin\alpha \cos\alpha \cos\phi + (s^2\lambda^{-1/2} + c^2\lambda)^2 \cos^2\alpha] \quad (14)$$

and

$$\cos^2\alpha' = \frac{R^2}{R'^2}[c^2s^2(\lambda - \lambda^{-1/2})^2 \sin^2\alpha \cos^2\phi + 2(s^2\lambda^{-1/2} + c^2\lambda)cs(\lambda - \lambda^{-1/2}) \sin\alpha \cos\alpha \cos\phi + (s^2\lambda^{-1/2} + c^2\lambda)^2 \cos^2\alpha] \quad (15)$$

Combining eqs 14 and 15 in evaluating eq 6 is formally equivalent to evaluating $\omega_0 R_0^{-2}$ 1/2 $\langle R_z'^2 2 - R_x'^2 - R_y'^2\rangle_{R,\cos\alpha,\phi}$. Noting further that $\langle R^2\rangle = R_0^2$, and allowing that for an initially isotropic distribution, the spherical polar averages yield $\langle\cos^2\alpha\rangle = {}^1/_3$, $\langle\sin^2\alpha\rangle = {}^2/_3$, $\langle\sin^2\phi\rangle = \langle\cos^2\phi\rangle = {}^1/_2$, and $\langle\cos\phi\rangle = 0$, it may be shown that the ensemble averaged splitting can be written

$$\langle\omega\rangle = \omega_0\frac{1}{3}\left(\frac{3}{2}c^2 - \frac{1}{2}\right)[\lambda^2 - \lambda^{-1}] \quad (16a)$$

In Figure 3a, we show examples of the angular dependences of the normalized splitting, $\Delta\omega/\omega_0$, calculated using eq 16a, for uniaxial deformations with λ values ranging from 1.0 to 2.0. In each case the mean splitting varies independently as $P_2(\cos\Theta)$ and $(\lambda^2 - \lambda^{-1})$.

For small strains, $\epsilon = \lambda - 1$, eq 16 reduces to

$$\langle\omega\rangle \approx \omega_0\epsilon\left(\frac{3}{2}c^2 - \frac{1}{2}\right) \quad (16b)$$

2.6. Mean Spectrum for Planar Biaxial Deformation. We now evaluate eq 6 under the deformation shown in eq 11, using rotation of the sample about the *y* axis as an example (see Figure 2b) so that

$$R_x' = (c^2 + s^2\lambda)R_x + cs(\lambda - 1)R_z$$
$$R_y' = \lambda^{-1}R_y$$
$$R_z' = cs(\lambda - 1)R_x + (s^2 + c^2\lambda)R_z \quad (17)$$

Thus

$$R^2 = R^2[(c^2 + s^2\lambda)^2 \sin^2\alpha \cos^2\phi + 2(c^2 + s^2\lambda)cs(\lambda - 1) \sin\alpha \cos\alpha \cos\phi + c^2s^2(\lambda - 1)^2\cos^2\alpha + \lambda^{-2} \sin^2\alpha \sin^2\phi + c^2s^2(\lambda - 1)^2 \sin^2\alpha \cos^2\phi + 2(s^2 + c^2\lambda)cs(\lambda - 1) \sin\alpha \cos\alpha \cos\phi + (s^2 + c^2\lambda)^2\cos^2\alpha] \quad (18)$$

and

$$\cos^2\alpha' = \frac{R^2}{R'^2}[c^2s^2(\lambda - 1)^2 \sin^2\alpha \cos^2\phi + 2(s^2 + c^2\lambda)cs(\lambda - 1) \cos\alpha \sin\alpha \sin\phi + (s^2 + c^2\lambda)^2\cos^2\alpha] \quad (19)$$

Again performing the ensemble average over R, $\cos\alpha$, and ϕ, we find that the ensemble averaged splitting may be written as follows:

Case I (Rotation about *y* (Squeeze) Axis).

$$\langle\omega\rangle = \omega_0\frac{1}{3}\left[-\frac{1}{2}(c^2 + s^2\lambda)^2 + \frac{1}{2}c^2s^2 + (\lambda - 1)^2 - \frac{1}{2}\lambda^{-2} + (s^2 + c^2\lambda)^2\right]$$
$$= \omega_0\frac{1}{3}\left[(\lambda^2 - 1)\frac{1}{2}(3c^2 - 1) + \frac{1}{2}(1 - \lambda^{-2})\right] \quad (20a)$$

For small strains, eq 20a reduces to

$$\langle\omega\rangle = \omega_0\frac{2}{3}\epsilon\left[\frac{3}{2}c^2\right] \quad (20b)$$

while for $\lambda \gg 1$ the expression for the average splitting returns to the Legendre polynomial angular dependence, $\langle\omega\rangle = \omega_0$ 1/3 $\lambda^2 P_2(\cos\Theta)$.

Case II (Rotation about *x* (Neutral) Axis). The case of rotation about the neutral axis is illustrated in Figure 2c. The ensemble-averaged splitting for this geometry may be written

$$\langle\omega\rangle = \omega_0\frac{1}{3}\left[-\frac{1}{2}(c^2\lambda^{-1} + s^2\lambda)^2 + \frac{1}{2}c^2s^2(\lambda - \lambda^{-1})^2 - \frac{1}{2} + (s^2\lambda^{-1} + c^2\lambda)^2\right]$$
$$= \omega_0\frac{1}{3}\left[(\lambda^2 - \lambda^{-2})\frac{1}{2}(3c^2 - 1) - \frac{1}{2}(1 - \lambda^{-2})\right] \quad (21a)$$

For small strains, eq 21a reduces to

$$\langle\omega\rangle = \omega_0\frac{2}{3}\epsilon\left[3c^2 - \frac{3}{2}\right] \quad (21b)$$

while for $\lambda \gg 1$ the expression for the average splitting again returns to the Legendre polynomial angular dependence, $\langle\omega\rangle = \omega_0{}^1/_3\lambda^2 P_2(\cos\Theta)$.

Equations 20 and 21 show that the angular dependences of the splitting are a function of the extension ratio, λ. The effect is illustrated for rotation about *y* and *x*, respectively, in Figure 3, parts b and c, where we show examples of the angular dependences of the splittings calculated using eqs 20 and 21, for biaxial deformations with λ values again ranging from 1.0 to 2.0. The contrast with Figure 3a is evident, the angular and strain dependences now being coupled. The deviation from $P_2(\cos\Theta)$ is strongest for small deformations, i.e., $\lambda \sim 1$. For $\lambda \gg 1$, both expressions yield $\langle\omega\rangle \sim P_2(\cos\Theta)$, an expected result since the deformation returns to uniaxiality in this limit.

2.7. Symmetric Hierarchy. In considering the system of deuterated probe molecules within a strained network, it is worth noting that there are a number of levels at which biaxiality can exist. First and foremost, the atomic nucleus is sensitive to the electric field

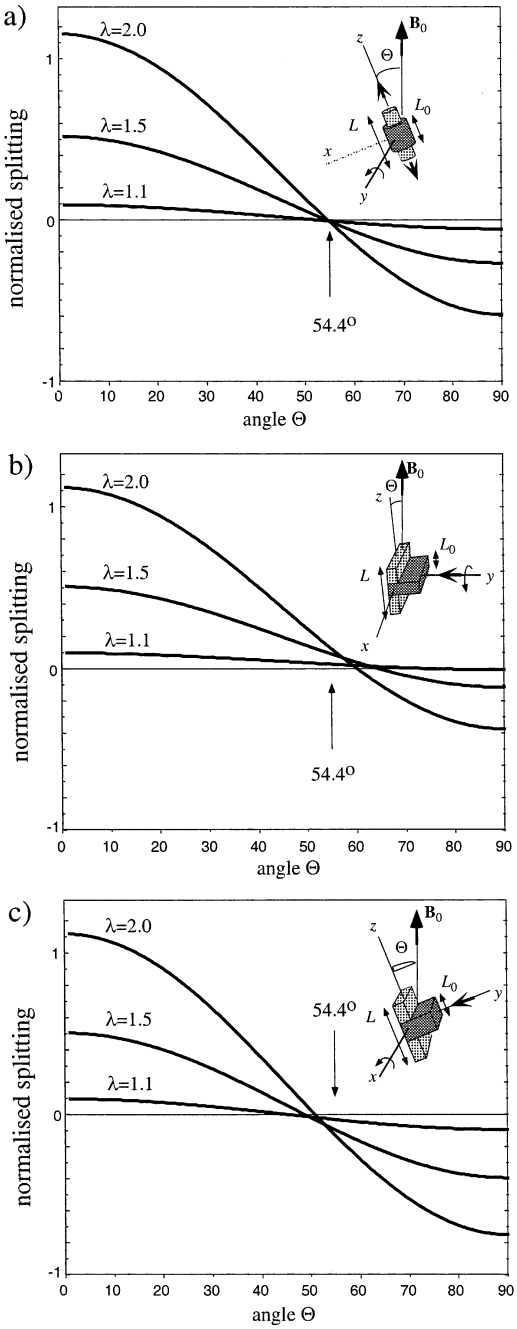

Figure 3. (a) Mean normalized splitting ($\Delta\omega/\omega_0$) derived from incompletely averaged second rank NMR interactions exhibited by solutes in uniaxially deformed networks following the well-known $P_2(\cos\Theta)$ dependence (eq 17) wherein, independent of the strain $\lambda = L/L_0$ (see inset), the interaction vanishes when the constraint director (*z*-direction) and the magnetic field $\mathbf{B}_o$ are at the "magic angle," $\Theta = 54.74°$. (b) Mean normalized splitting ($\Delta\omega/\omega_0$) derived from incompletely averaged second rank NMR interactions exhibited by solutes in biaxially deformed networks that cannot be factored into strain-dependent and angular-dependent contributions (eq 24) and where the $P_2(\cos\Theta)$ dependence no longer applies. (c) For rotation of constraint director (*z*-direction) in the $x-z$ plane (see inset), where the interaction vanishes when the inclination angle exceeds the "magic angle" and $\Theta = 54.74°$ and is a function of the strain $\lambda = L/L_0$. For rotation of constraint director (*z*-direction) in the $y-z$ plane (see inset), the interaction vanishes when the inclination angle is less than the "magic angle," $\Theta = 54.74°$ and is a function of the strain $\lambda = L/L_0$.

gradient tensor, whose biaxiality is normally accounted for in the asymmetry parameter,[18] η. The symmetry of the efg depends on the local bond symmetry, which in the case of the C−D bonds of the methyl groups of the PDMS oligomer used in this study, is cylindrical, leading to $\eta = 0$. Also, $\eta < 0.1$ for the aromatic deuterons of the 1,2-dichrobenzene-d_4, which we also report on in the Experimental Section.

At a higher level the probe molecule that contains the relevant C−D bond may itself break cylindrical symmetry, and thus possess inherent shape biaxiality. Neither the PDMS oligomer nor the 1,2-dichrobenzene-d_4 are uniaxial molecules. Further, the local "director" about which the probe molecule effectively orients through biased steric interactions, may not be uniaxial. In the network example, that director corresponds to the PDMS chain tethered between cross-links; the chain will be biaxial at the segment level but, averaged over all segments, may approximate uniaxiality. In this work, we shall be concerned with the manner in which the probe molecule and tethered chain symmetries are mutually expressed via the probability distribution of probe molecule orientation with respect to the director frame which is defined by **R**. This distribution will depend in a subtle manner on the outcome of steric influences on probe molecule dynamics and will be difficult to calculate. However we can, and will, allow for biaxiality in that distribution.

Finally we must deal with the symmetry of the strained network that provides the molecular environment—the diffusion-averaged constraint on the mobile probe. We shall show that it is this symmetry that dominates the angular dependence of the deuteron NMR spectra.

2.8. The Quadrupolar Spin Hamiltonian for a Probe Molecule in an Ordered Matrix. We will show that, because of motional averaging, only biaxiality in the network deformation will be seen in the angular dependence of the splitting. To understand the details of the symmetry hierarchy, it is helpful to write down the full quadrupolar Hamiltonian for a nuclear spin present in a molecule undergoing anistropic motion. This requires that we write an exact form for the Hamiltonian, starting at the frame of the molecule and transforming sequentially to the laboratory frame. Our starting point is the case of a probe molecule embedded in a liquid crystal matrix[21,23] whose director has some specific orientation with respect to the magnetic field.

Luz and Meiboom[23] present a formalism appropriate to probe molecules in a liquid crystal matrix, whereby the efg is described in a (primed) molecular frame the angular distribution of the molecule is described in an (unprimed) host matrix frame of fixed orientation with respect to the magnetic field, while the magnetic field itself defines the (double primed) good quantum number frame. The quadrupole spin Hamiltonian in the molecular frame is expressed via a spin operator T and a spherical tensor, F, that describes the efg, as[23]

$$H^{(2)} = \sum_{p=\pm 2,0} (-1)^p F'^{(2)}_p T'^{(2)}_{-p} \qquad (22)$$

Note that $F'^{(2)}_0$ arises from the V_{zz} principal axis term of the efg, while the $F'^{(2)}_{\pm 2}$ arise from the asymmetry parameter of the efg. Rewriting eq 22 in the laboratory frame, Luz and Meiboom obtain

$$H^{(2)} = \sum_{p,q,n} (-1)^p F'^{(2)}_p D^{(2)}_{q,-p}(\Omega) D^{(2)}_{n,q}(\Omega_{B_0}) T''^{(2)}_n \qquad (23)$$

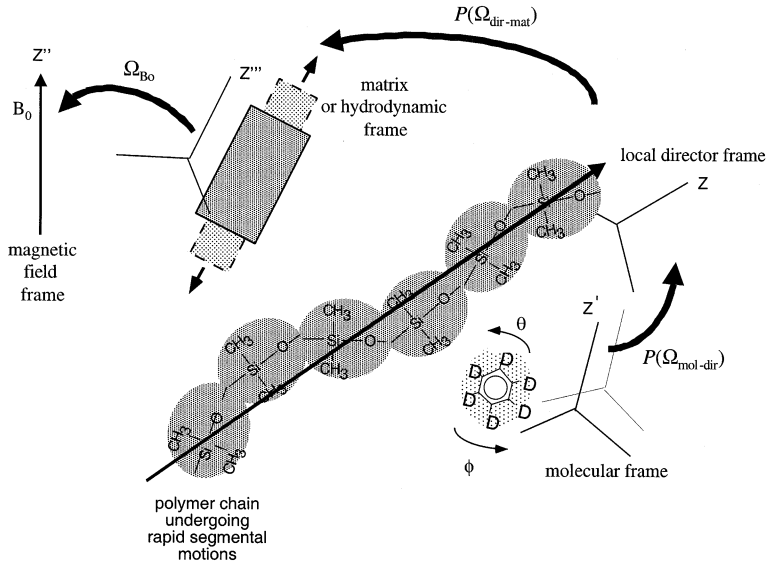

Figure 4. Schematic representation of the succession of rotations from the frame of reference of the deuterated probe molecule (primed) to the local polymer chain director (unprimed) to the elastomer deformation frame (triple primed) to the laboratory magnetic field frame (double primed).

For rapid probe molecule tumbling, eq 23 is averaged over all molecular orientations Ω using an angular distribution of the molecule in the host matrix frame is expressed as an expansion of Wigner rotation matrixes,[24] i.e.

$$P(\Omega) = \sum_{L,k,m} \frac{(2L+1)}{8\pi^2}(-1)^{k-m} C^{(L)}_{k,m} D_{k,m}{}^{(L)}(\Omega) \quad (24)$$

An axially symmetric distribution will be represented by $C^{(L)}_{k,m} = 0$ for k or m nonzero. Further, we note that in the case of a system which is symmetric under inversion (eg the nematic systems considered in this article) $C^{(L)}_{k,m} = 0$ for k or m odd.

The quadrupole interaction spin Hamiltonian, after the appropriate transformations from the molecular frame via the matrix frame to the lab frame, and on taking the secular part only in accordance with first-order perturbation requirements, is given by[23]

$$\bar{H}^{(2)} = \left\{ \sum_{q=0,\pm2} \left[\sum_{p=0,\pm2} (-1)^p F'^{(2)}_p C^{(2)}_{-q,p} \right] D_{0,q}{}^{(2)}(\Omega_{B_0}) \right\} T'^{(2)}_0 \quad (25)$$

where $T'^{(2)}_0$ is the usual $3I_z{}^2 - 1$ operator in the lab frame and Ω_{B_0} describes the orientation of the host matrix in the magnetic field frame. $D^{(2)}_{0,0}(\Omega_{B_0})$ gives the $P_2(\cos\Theta)$ dependence while $D^{(2)}_{0,\pm2}(\Omega_{B_0})$ gives the $\sin^2\Theta\cos 2\Phi$, $\sin^2\Theta\sin 2\Phi$ terms, which we associate with the biaxial part of the angular response. Note that irrespective of the symmetry of the efg (i.e. the parameter p) a biaxial angular distribution of the splitting requires $C^{(2)}_{\pm2,p} \neq 0$, i.e., a nonaxially symmetric angular distribution for the molecule. For completeness, we relate the $C^{(2)}_{-q,p}$coefficients to the Saupe order parameters.[25] $\langle S\rangle = \langle S_{z'z'}{}^{zz}\rangle$ contributes to $C_{0,0} \neq 0$ only, $\langle D\rangle = \langle S_{z'z'}{}^{xx} - S_{z'z'}{}^{yy}\rangle$ contributes to C$\pm$2,0 $\neq 0$ only, $\langle S_{x'x'}{}^{zz} - S_{y'y'}{}^{zz}\rangle$ contributes to $C_{0,\pm2} \neq 0$ only and $\langle S_{x'y'}{}^{xy}\rangle$ contributes to $C_{\pm2,\pm2} \neq 0$ only.

2.9. The Quadrupolar Spin Hamiltonian for a Probe Molecule in an Elastomer. We now adapt the approach of Luz and Meiboom[23] to the problem under present consideration. Our system has one additional level in the hierarchy, since rather than experiencing a unique local matrix frame (the local polymer segment director), the probe molecule, through rapid diffusion over many chains, yields an average over all directors. In the simple formalism of eq 3, this corresponds to an average over all $\Delta\omega(R',\cos\alpha')$. To handle this problem in the language of Luz and Meiboom we must decompose the angular distribution coefficient $C^{(L)}_{k,m}$ by allowing a two-stage motional averaging, first from the molecular frame to the local chain director, via an angular distribution $P^{\mathrm{mol-dir}}(\Omega_{\mathrm{mol-dir}})$ and then from the chain directors to the matrix frame via an angular distribution $P^{\mathrm{dir-mat}}(\Omega_{\mathrm{dir-mat}})$, the new matrix frame now being the principal axis frame for the elastomer extension.

This is performed in the following way. First we note that the Hamiltonian transformation represented by eq 23 has an additional rotation. The succession of rotations is shown in Figure 4. Instead of a single transformation from the molecular to the single matrix-director frame as represented by the rotation matrix $D^{(2)}_{q,-p}(\Omega)$ we now require a matrix product representing the successive steps $\Omega_{\mathrm{mol-dir}}$ and $\Omega_{\mathrm{dir-mat}}$. This means that $D^{(2)}_{q,-p}(\Omega)$ is replaced by $\sum_j D^{(2)}_{q,j}(\Omega_{\mathrm{dir-mat}}) D^{(2)}_{j,-p}(\Omega_{\mathrm{mol-dir}})$.

Next we define the two independent angular distributions,

$$P^{\mathrm{dir-mat}}(\Omega_{\mathrm{dir-mat}}) = \sum_{L,k,m} \frac{(2L+1)}{8\pi^2}(-1)^{k-m} C^{\mathrm{dir-mat}(L)}_{k,m} D^{(L)}_{k,m}(\Omega_{\mathrm{dir-mat}}) \quad (26)$$

and

$$P^{\mathrm{mol-dir}}(\Omega_{\mathrm{mol-dir}}) = \sum_{L',k',m'} \frac{(2L+1)}{8\pi^2}(-1)^{k'-m'} C^{\mathrm{mol-dir}(L')}_{k',m'} D^{(L')}_{k',m'}(\Omega_{\mathrm{mol-dir}}) \quad (27)$$

Integrating over all orientations and making use of the orthonormality relations for the Wigner matrices, we find that eq 25 is unchanged except that we now replace $C^{(2)}_{-q,p}$ by

$$C^{(2)}_{-q,p} = \sum_j C^{\mathrm{dir-mat(2)}}_{-q,j} C^{\mathrm{mol-dir(2)}}_{j,p} \tag{28}$$

Again we emphasize that eq 25 dictates that irrespective of the parameter p, a biaxial angular distribution of the splitting requires $C^{\mathrm{dir-mat(2)}}_{\pm 2,j} \neq 0$ for some value of j for which $C^{\mathrm{mol-dir(2)}}_{j,p} \neq 0$. This implies that whatever the symmetry of the efg (i.e., the value of the parameter p), or the probe molecule (i.e. the value of the parameter j), biaxiality in the angular dependence of the quadrupole splitting will only be observed if it is present in the highest level of the hierarchy, namely the angular distribution of the directors with respect to the matrix. Furthermore, biaxiality in either the efg or the molecule-director angular distribution will only contribute to biaxiality in the angular dependence of the quadrupole splitting via Saupe parameters for $C^{\mathrm{mol-dir(2)}}_{j,\pm 2}$ and $C^{\mathrm{dir-mat(2)}}_{\pm 2,j}$ respectively of higher order than $\langle D \rangle$ and thus they participate only to second order. Thus, we do not expect to see a significantly greater splitting when a biaxial rather than uniaxial probe molecule is employed.

Finally, we return to eq 3 and relate that expression to the Luz and Meiboom formalism. Equation 3 asserts the quadrupole splitting prior to any diffusive averaging by the probe molecule of the director distribution. It is therefore best approached by assuming a fixed director inclined at Ω_{B_0} to the magnetic field. Thus, eq 25 becomes

$$\bar{H}^{(2)} = \left\{ \sum_{q=0,\pm 2} \left[\sum_{p=0,\pm 2} (-1)^p F'^{(2)}_p C^{\mathrm{mol-dir(2)}}_{-q,p} \right] D^{(2)}_{0,q}(\Omega_{B_0}) \right\} T''^{(2)}_0 \tag{29}$$

Equation 3 is returned if and only if $C^{\mathrm{mol-dir(2)}}_{-q,p} \neq 0$ only for $p = q = 0$. This implies cylindrical symmetry about the director axis in the sampling of orientation by the probe molecule. We shall return to this point in the discussion.

3. Experiment

We have carried out deuteron NMR spectroscopy experiments at both 60 and 45 MHz using the signal from a deuterated probe molecule diffusing within a cross-linked PDMS network. This probe was, in one set of experiments, perdeuterated poly(dimethylsiloxane) (PDMS) oligomer ($M \sim$ 10 kDa) while in a second set, 1,2-dichrobenzene-d_4 was used. The network sample was biomedical grade silicone sheeting, obtained from Speciality Manufacturing (Saginaw, MI) in the form of a sheet of 1.5 mm thickness. The sample to be deformed was cut into a rectangular cuboid and a small drop of the oligomer placed on the surface and dissolved to give a sample with ~7 wt % of oligomer to network. Once the probe molecules had diffused completely into the sample, the surface was wiped and the sample dimension was trimmed to match the exact lateral dimension of the cells corresponding to the neutral axis, and then placed in one of two compression devices shown in Figure 5.

The system shown in Figure 5a was used for rotating a compressed sample around the *squeeze* axis so that the magnetic field lies at a chosen angle in the plane of the *stretch-neutral* axes. This device was made of delrin and could be contained entirely within the solenoidal rf coil used for the NMR experiments. The delrin vice enabled the network sample to be compressed by a known ratio λ^{-1} while one transverse dimension remained fixed. The sample freely expanded along the remaining extension direction with excess sample protruding beyond the ends of the vice being trimmed as required. The vice could be rotated to allow the sample to be reoriented in the $x-z$ (*neutral axis-stretch axis*) plane. This system was employed in the experiments carried out at Chapel Hill, in the 60 MHz spectrometer.

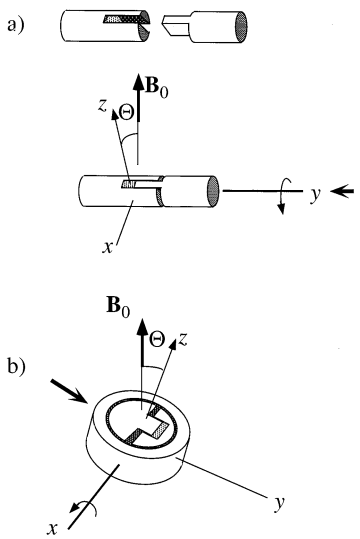

Figure 5. (a) Schematic diagram of the Delrin "tab-in-slot" compression vice which biaxially deforms a rubber network. The z axis of the strain tensor describing the deformation is along the extrusion direction. The cylindrical vice is inserted into a solenoidal rf coil and the angle between z axis and the magnetic field (Θ) is varied. (b) Schematic diagram of the Teflon compression vice used to rotate the extension axis z around the neutral (x) axis. The entire assembly is rotated inside a saddle rf coil.

In contrast, the device shown in Figure 5b was used for rotating a compressed sample around the *neutral* axis. This system was made of Teflon and was contained within a larger saddle coil. The Teflon vice also allowed sample compression while keeping one dimension fixed, the sample again freely extending and being trimmed as necessary. This latter device was used for the 45 MHz experiments carried out in Wellington.

Two approaches were used to obtain spectra from which the quadrupole splittings could be derived. The first (one-dimensional method) consisted of a simple free induction decay (FID) acquisition following a single 90° rf pulse. Examples of NMR spectra obtained at 60 MHz by this method using 64 acquisitions are shown in Figure 6 for $\lambda = 2.04$. The second (two-dimensional method) involved the use of a simple (Hahn) echo comprising a 90_x-180_y-acquire rf pulse train in which the echo evolution time was varied. The data could then be Fourier transformed with respect to both evolution and evolution times, to yield a 2-dimensional spectrum in which that arising in the evolution domain was free of any Zeeman broadening due to susceptibility artifacts. We found that both methods gave identical splitting but with greater spectral resolution being available in the 2D method.

In the cases of rotation about the *squeeze* axis, spectra were obtained for 4 different compression ratios using 12 different orientations between 0 (stretch axis along field) and 90° (neutral axis along field). Similar angular steps were used in the case of rotation about the *neutral* axis and again, spectra were obtained for four different compression ratios. The errors in determining the angle was estimated at ±1° in the cell used for rotation about the *squeeze* axis and around ±1.5° in the cell used for rotation about the *neutral* axis. Best estimates of the extension ratios were obtained by measurement, before and after squeezing, of the sample thicknesses in the squeeze

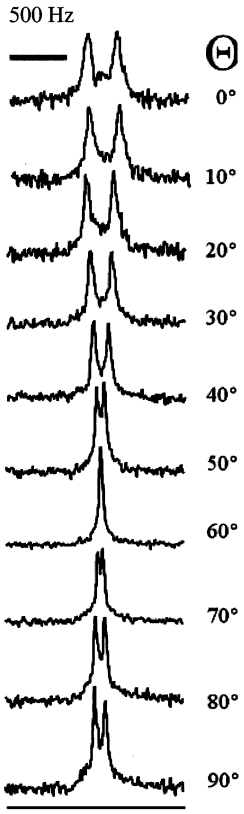

Figure 6. Angular dependent deuterium NMR spectra of PDMS-d_6 oligomer in a biaxially compressed PDMS network with $\lambda = 2.04$.

directions, and the sample lengths in the stretch directions. These measurements of λ were estimated to be accurate to within ±5%.

4. Results

The system shown in Figure 5a was used for rotating a compressed sample around the *squeeze* axis. Spectra were analyzed for four different compression ratios of 1.27, 1.45, 1.79, and 2.04, in each case using 12 different orientations between 0 (stretch axis along field) and 90° (neutral axis along field). In the vicinity of the splitting null points, angular steps were taken at closer intervals. The angular dependences along with the predictions of eq 20a are shown in Figure 7. Only one parameter common to the entire set was adjusted, namely the splitting parameter, ω_0. The family of calculated curves shown in Figure 7 represent the best fit to the entire data set, resulting in a value of $\omega_0/2\pi = 216$ Hz. The remaining discrepancies between the theory and data arise from uncertainties in the experimental value of λ. The data shown in Figure 6 deviate significantly from a $P_2(\cos\Theta)$ dependence, a point which is emphasized by the displacements of the splitting null points from 54.4° as indicated by the arrows in the diagram. The shifts of these null points agree well with the predictions of eq 20a.

Figure 8 shows the angular dependences of splittings obtained in the cell used for rotation about the *neutral* axis (see Figure 5b). Four extension ratios, estimated at 1.26, 1.37, 1.65, and 1.94, were used. Again the data exhibit a distinct deviation from $P_2(\cos\Theta)$ behavior, with splitting null points displaced from 54.4°. By contrast with the case of rotation about the *squeeze* axis shown in Figure 7, these null points for the data in Figure 8 are displaced to lower angle. The corresponding theo-

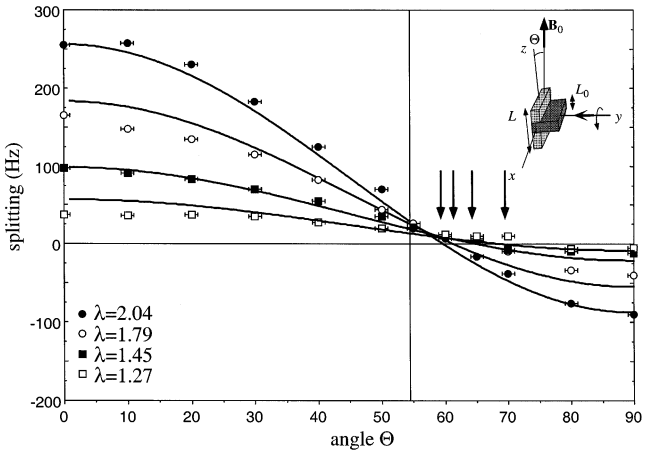

Figure 7. Experimental and theoretical (solid curve) mean splittings of theangular dependent deuterium NMR spectra (PDMS-d_6 oligomer in a biaxially compressed PDMS network) as a function of λ in the case of rotation of the constraint director (z-direction) in the $x-z$ plane (see inset). The arrows indicate the angular positions of splitting nulls.

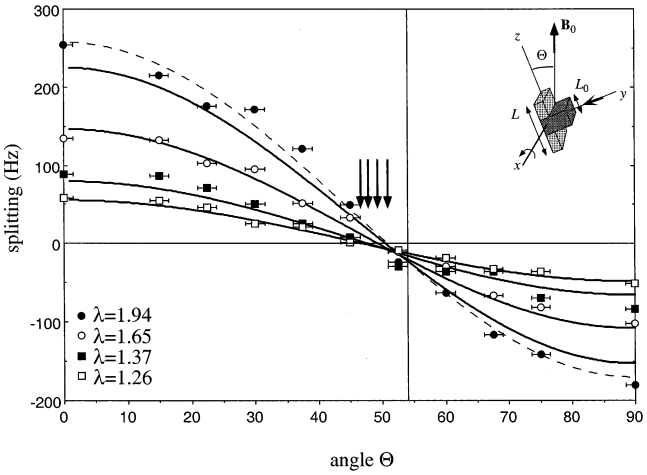

Figure 8. Experimental and theoretical (solid curve) mean splittings of theangular dependent deuterium NMR spectra (PDMS-d_6 oligomer in a biaxially compressed PDMS network) as a function of λ in the case of rotation of the constraint director (z-direction) in the $y-z$ plane (see inset). The arrows indicate the angular positions of splitting nulls. The dashed line shows a better fit to the $\lambda = 1.94$ data obtained by adjusting the estimated value of λ to 2.05.

retical expression for rotation about the *neutral* axis is given by eq 21a. The predictions of this equation based on the estimated extension ratios, are also shown in Figure 8, with vertical arrows used to indicate splitting nulls. This family of curves were calculated using the same splitting parameter value ($\omega_0/2\pi = 216$ Hz) found in the data shown in Figure 7 for rotation about the *squeeze* axis. Again the agreement is good, given the uncertainty in the measured value of λ. The poorest agreement was found for the largest extension ratio, $\lambda = 1.94$. A significantly improved fit results if one allows a 5% higher value for λ.

The deuterated oligomer used in this work comprises on the order of 20 Kuhn statistical segments. The rotational mobility of these segments, along with the very short segmental correlation time ensures that the oligomer exhibits axial symmetry on the characteristic time scale of the NMR spectrum (>10 μs). To investigate the role of probe molecule biaxiality, we have carried out measurements of the quadrupole splitting for 1,2-dichlorobenzene-d_4 in the biaxially deformed PDMS

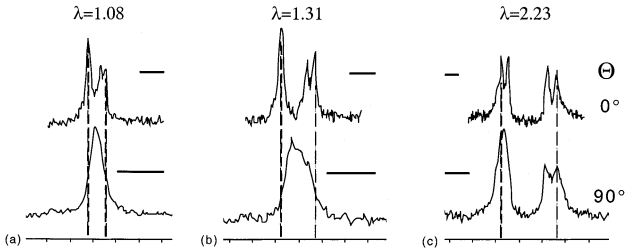

Figure 9. Mean quadrupolar splittings of the biaxial solute 1,2-dichlorobenzene-d_4 in a biaxially deformed PDMS networks at two orientations $\Theta = 0$ and 90°. The scale bar is 100 Hz; the abcissa of the $\Theta = 0°$ spectra is contracted by a factor of 2 in order to facilitate a comparison at these extreme orientations.

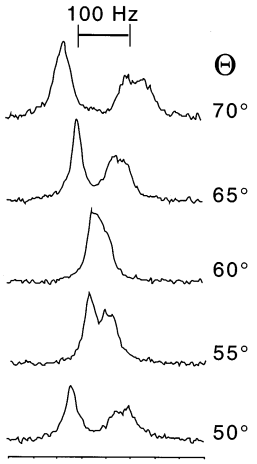

Figure 10. Θ dependence of the mean quadrupolar splittings of 1,2-dichlorobenzene-d_4 in a biaxially deformed PDMS network ($\lambda = 2.23$) near the zero-crossing. Within experimental resolution uncertainties, there is no evidence for different zero-crossings for the two different quadrupolar interactions although in theory this is possible (see the Appendix from ref 23).

networks, using different orientation angles in the case of rotation about the *squeeze* axis. Three different extension ratios of 1.08, 1,31, and 2.23 were used. The spectra obtained were necessarily more complex, because of the combination of different chemical shifts and different quadrupole splittings at the two chemically distinct (ortho- and para-*)* deuteron sites. This complexity makes it difficult to extract unique splittings at all orientation angles. However we can learn a great deal by comparing spectra obtained at the two orientation extremities (at $\Theta = 0°$ and $\Theta = 90°$) and near the splitting null. These are shown respectively in Figure 9 for all three values of the extension ratio and in Figure 10 for a range of angles near 60° for $\lambda = 2.23$. A $P_2(\cos \Theta)$ splitting dependence associated with uniaxial behavior would predict a factor of 2 scaling in the spectra at $\Theta = 0°$ and $\Theta = 90°$. In Figure 9, we superpose scaled spectra obtained at $\Theta = 0°$ and $\Theta = 90°$ and observe an expected clear deviation from $P_2(\cos \Theta)$ behavior, again most apparent when the extension ratio λ is close to unity. The spectra shown in Figure 10 are especially interesting because a common splitting null is found near $\Theta = 60°$. The biaxial character of the probe molecule does, in principle, allow for different angular dependences at different deuteron sites.[23] No such behavior is apparent here. Indeed the 1,2-dichlorobenzene-d_4 probe returns behavior similar to that observed for the deuterated oligomer of PDMS.

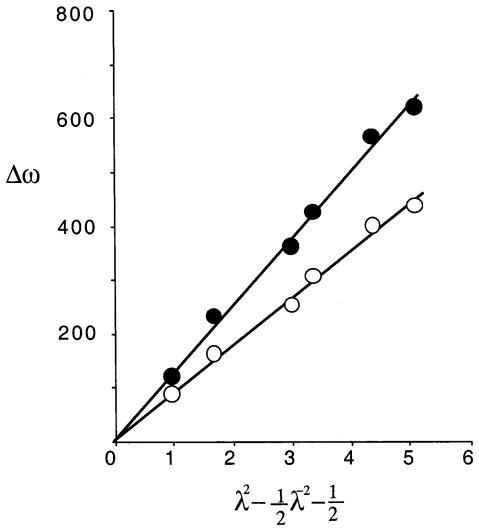

Figure 11. Strain dependence of the mean quadrupolar splittings of 1,2-dichlorobenzene-d_4 in a biaxially deformed PDMS network at $\Theta = 0°$ (eq 24); the larger splitting derives from the equivalent *para*-deuterons (closed circles); the equivalent *ortho*-deuterons (open circles) exhibit a weaker λ dependence.

At $\Theta = 0°$ the ortho- and para-deuteron spectra are well resolved and splittings were able to be measured over a wide range of extension ratios, λ. These are shown in Figure 11. They precisely follow the prediction of eq 20a for $\cos \Theta = 1$, i.e.

$$\langle \omega \rangle = \omega_0 \frac{1}{3}\left[\lambda^2 - \frac{1}{2} - \frac{1}{2}\lambda^{-2}\right] \qquad (30)$$

In all the experiments reported here, the deuterium quadrupole interaction is reduced by several orders of magnitude due to the tumbling motion of the probe molecule. The sensitivity of the probe molecule to the chain orientation, in the case of a network end-to-end vector **R** is given (see eq 3) by the ratio of ω_0 to the static probe molecule quadrupole splitting. The static ^{2}H NMR quadrupole interaction for deuterated methyl groups in PDMS is known to be 175 kHz[26] while the quadrupole splitting is ≈100 Hz, a scaling factor of 5×10^{-4}.

5. Discussion

Previous experiments[1,2,5] on deuterated probe molecules in uniaxially deformed elastomers have shown good agreement with the predictions of the simple phantom Gaussian chain model, based on the idea of a "pseudo-nematic" interaction in which the probe inherits some fraction of the order experienced by the polymer chains comprising the matrix. In the present work, we have used a biaxial deformed network to provide a more complex and detailed test of the model. In particular, the angular variations of the splittings observed here agree well with the predicted dependence on extension ratio λ. Further agreement is found with the predicted λ dependence at fixed orientation $\Theta = 0°$. We note that these results hold whether or not the probe molecule itself exhibits biaxial properties.

The present work therefore raises a number of interesting questions. First, why do we see a behavior which is independent of probe molecule symmetry? Second, how can we distinguish between the angular dependence of spectral behavior observed from a molecule whose deuteron efg is inherently biaxial and the

angular dependence of one in which the host environment is biaxial? Third, is the angular dependence observed in biaxial deformation, a measure of the statistical physics model used to depict the chains? Finally, why does the phantom chain model work so well, when it clearly fails to predict the elastomeric mechanical properties? We address these questions in turn.

5.1, The Symmetry of the Probe Molecule. The characteristic time scale ($\sim 10\ \mu$s) set by our experiment is determined by the strength (in frequency units) of the electric quadrupole interaction, of around 200 kHz. This rate is further reduced by the motional averaging associated with the reorientation of the probe molecule as it undergoes the rotational diffusion of Brownian tumbling, making the effective time scale of the interaction in excess of 1 ms. This "interaction rate" is much slower than the polymer chain segmental reorientation. Fast, localized processes such as intra-monomer vibrations and correlated conformer isomerizations have time scales on the order of 10^{-12} to 10^{-9} s and are comparable to motions in simple liquids. On the length scale of the network chain end-to-end vector, the connectivity of monomers leads to the Rouse modes[27] which may exhibit dynamics on the microsecond time scale. Thus, in experiencing the steric effects of collisions with the polymer chains, the diffusing probe molecule will rapidly sample all possible monomeric orientations associated with the segmental motion of the tethered chain, so that a quadrupole interaction time-averaged over these motions will be experienced. Further, one may argue that the fast segmental reorientation around the director axis leads to a distribution of monomeric orientations that is cylindrically symmetric with respect to the axis of the mean chain director, **R**. Whatever the shape of the probe molecule, this cylindrical symmetry will be reflected in the averaged probe molecule orientation. In consequence, we expect $C_{j,p}^{\mathrm{mol-dir}(2)} \neq 0$ only for $j = p = 0$. This leads to a significant simplification of eq 28 in which $C_{-q,0}^{(2)} = C_{-q,0}^{\mathrm{dir-mat}(2)}\, C_{0,0}^{\mathrm{mol-dir}(2)}$ and $C_{-q,p}^{(2)} = 0$ for $p \neq 0$. Thus, the observed quadrupole interaction symmetry derives entirely from the matrix director distribution and the measured order parameter is directly proportional to the matrix with scaling factor $C_{0,0}^{\mathrm{mol-dir}(2)}$. We further note that the result $C_{j,p}^{\mathrm{mol-dir}(2)} \neq 0$ only for $j = p = 0$ is consistent with eq 3.

5.2. Apparent Biaxiality. It is reasonable to ask whether one might naively represent the splitting, at least mathematically, by adopting the expression for the quadrupole splitting for a molecule of fixed orientation, under conditions of a biaxial efg, and assuming some "pseudoasymmetry parameter" η. This splitting is given by[18]

$$\langle\omega\rangle = \omega_0\left[\frac{1}{2}(3c^2 - 1) + \eta\frac{1}{2}s^2\cos 2\Phi\right] \qquad (31)$$

where Φ is the azimuthal angle of the magnetic field direction in the efg principal axis frame and $\eta = (V_{xx} - V_{yy})/V_{zz}$. Equation 31 appears at first sight to have a slightly different angular dependence from that of eqs 20 and 21. However, by simple rearrangement it may be easily shown that these equations are equivalent if we set $\eta = 3/2(1 - \lambda^{-2})/(\lambda^2 - (1)/(2) - (1)/(2)\lambda^{-2})$ and, for the case of rotation about y (the squeezed axis), take $\Phi = 0$, while for rotation about x (the neutral axis), take $\Phi = 90°$. η reduces to unity for small strains, and zero for $\lambda \gg 1$ and hence is strain-independent in these limits.

The apparent similarity between the angular dependence expressed in eqs 20 and 21 and eq 31 is purely formal. In practice, whatever the source of biaxiality, whether in the efg, in the probe molecule geometry, or in the surrounding matrix, provided that the deviation from isotropy is small, the angular dependence of the quadrupole splitting can always be expressed through a superposition of terms as represented by eq 31. This superposition is a consequence of the quadratic dependence on cos Θ and sin Θ and the formal similarity serves to indicate that for small distortions, mere angular dependence does not define the physical source of biaxiality, but rather the symmetry. For large distortions, however, the existence of formal similarity will depend on the model that connects the quadrupole splitting to the chain deformation.

5.3. The Significance of the Elastomeric Model for the Order Parameter. The angular dependence of the splitting does depend on the underlying elastomeric physics. In the present case we use the Sotta and Deloche expression for the splitting $\Delta\omega$, in which a quadratic dependence on cos Θ and sin Θ is implicit. In contrast, consider the trivial case in which eq 3 is modified to allow for an additional term in $\Delta\omega$ independent of chain length or orientation. Clearly the resulting angular dependence of the observed splitting would deviate from that given in eq 22. Of more physical interest might be the inclusion of a term quartic in the chain length, with eq 3 modified to read

$$\Delta\omega = \omega_0\left\{\left(\frac{R}{R_0}\right)^2 + \alpha\left(\frac{R}{R_0}\right)^4\right\}P_2(\cos\alpha) \qquad (32)$$

We now have the task of evaluating $\langle(R'/R_0)^4 P_2(\cos\alpha')\rangle_{R',\cos\alpha'}$. The resulting expression is given in the appendix for the case of a biaxial deformation and with rotation about y (squeeze) axis). It is clear that for large strains ($\lambda \gg 1$) it involves terms quartic in cos Θ and sin Θ and the consequential angular dependence of the splitting is different from that seen in eq 31. For small strains, however, the expression reduces to the identical $\cos^2\Theta$ dependence of 20b so that no evidence for quartic dependence of splitting on chain length is obvious from a measurement of angular dependence in the case of a weak perturbation.

In summary, it is in the details of the combined dependence of the quadrupole splitting on the strain λ and the angle Θ that evidence for the physical basis of the interaction can be elucidated. In the case of a probe molecule in a deformed network the angular dependence of the splitting will be overwhelmingly dominated by the elastomer properties and will depend on probe molecule or electric field gradient asymmetry only to second order.

5.4 NMR and mechanical measurements. It is well-known that the simple theory of rubber elasticity based on a phantom Gaussian chain model breaks down substantially for finite strains, and certainly for extension ratios on the order of those employed in this work. This model predicts both for the mechanical stress and the NMR quadrupole splitting, and dependence on uniaxial extension ratio as $(\lambda^2 - \lambda^{-1})$ and while this simple relationship holds in the case of NMR for λ values up to around 2.5, it breaks down[28] for elastic stress at around $\lambda \approx 1.5$. The reason for this discrepancy

most likely lies in the different details of the ensemble averages to which the measurements are sensitive, and especially the degree to which the methods are sensitive to finite chain length. In the case of mechanical extension the stress will be strongly influenced by a very few fully extended chains whereas these few chains will have little influence on the average order parameter as measured by NMR. NMR order parameters, as detected using rapidly diffusing probe molecules, will be strongly influenced by the behavior of the majority of the chains, for which the phantom Gaussian chain model works quite well. In contrast, the mechanical stress will be very sensitive to the deviant behavior of a few chains. It should be noted that other NMR experiments may well be more sensitive such deviations. In particular, where deuterons are placed on the polymer chains themselves, the effects of excluded volume and the inability of chains to pass through one another may well become apparent in the NMR spectrum.

6. Conclusions

By employing biaxial deformation we have been able to provide a more detailed NMR test of local ensemble-averaged order in elastomers, as measured by a rapidly diffusing deuterated probe molecule. The deuterium NMR experiment yields a splitting that depends on the time-averaged strength of the quadrupole interaction, as projected in the magnetic field frame of reference. By varying the orientation of biaxially deformed samples with respect to the magnetic field, we measure the angular dependence of the quadrupolar splitting at different strains. We show here that the phantom Gaussian chain model gives a good representation for the quadrupolar splitting which in turn provides a well-defined measure of chain order.

An analysis of the detailed averages associated with the time scale and orientational hierarchy over which probe molecule motion must be considered, indicates that the electric quadrupole interaction associated with a deuteron sited on the probe molecule, provides a well-defined measure of chain order. Consideration of this averaging process suggests that only biaxiality at the highest level of the hierarchy, namely in the distribution of chain end-to-end vectors, will be observed in the angular dependence of the splitting. This conclusion is supported by experiments performed as part of this work in which a nonaxially symmetric probe molecule returns the same behavior as exhibited by the (motionally averaged) axially symmetric oligomer.

A very different test of the chain statistics would be provided by a measurement of quadrupole splittings for deuterons that label the polymer chains themselves. In this case one observes an average of spectra obtained from every site, rather than an average interaction Hamiltonian, as is the case in this work. For a phantom Gaussian chain model, no quadrupole splitting is predicted, but rather a "super-Lorentzian" line[29,30] whose width depends on extension ratio. Nonetheless, under uniaxial extension splittings have been observed,[10,12] suggesting that chain labeling may provide a more sensitive indicator of deviations from the simple model. Indeed, modifications to the phantom chain model to allow for contributions from chain interactions have been shown to produce a splitting.[12] The difficulty with experimental studies using deuterium labeled chains is the need to avoid the effect of labeled dangling chains, whose spectral response is likely to be very similar to that of a freely diffusing probe molecule.

Our work has potential significance in relation to recent NMR experiments[17] on the use of deformed gels to orient protein molecules. In these latter NMR experiments protein secondary structure is elucidated through the use of orientationally dependent intramolecular dipolar interactions. We suggest that biaxial deformation of the host gel may prove useful in providing additional insight, for example concerning the complete angular coordinates of internuclear vectors. We note, however, that motional averaging considerations are crucial. In particular, and in contrast to the probe molecules used in this work, the proteins may need to be sufficiently large that their dimensions are comparable with the elastomer chains thus ensuring that the azimuthal orientation of the protein around the axis of the local chain director is correlated with the laboratory frame of reference.

Finally we note that the methods demonstrated here for elastomers under fixed strain, can be applied to molecules undergoing shearing flows. We further note that biaxial deformation is inherent to such flows, due to the lack of physical equivalence of the hydrodynamic velocity, gradient, and vorticity directions. For example, biaxiality leads directly to the second normal stress difference in the case of polymer melts undergoing shear flow.[31,32] Thus, we hope that our results may provide some further insight regarding the more general use of Rheo-NMR methods to measure molecular order under deformational flow.

Acknowledgment. E.T.S. wishes to acknowledge support from the National Science Foundation (DMR-9971143) and the John Simon Guggenheim Foundation; P.T.C. acknowledges support from the New Zealand Foundation for Research, Science and Technology, The Royal Society of New Zealand Marsden Fund, and the Centres of Research Excellence Fund. We also thank Julia Kornfield for valuable discussions regarding deviations from the $(\lambda^2 - \lambda^{-1})$ stress dependence for rubber elasticity, Rob Tycko for insights into the potential utility of biaxially strained networks, and Brad Douglass for his design of the deformation cell shown in Figure 5b.

Appendix A

The following expression gives the angular dependence of splitting for biaxial deformation where a quartic dependence on chain length is incorporated. The rotation axis is taken to be case I, in which rotation takes place about the *y* (*squeeze*) axis.

$$\langle\omega\rangle = \omega_0\frac{1}{3}\left[(\lambda^2-1)\frac{1}{2}(3c^2-1)+\frac{1}{2}(1-\lambda^{-2})\right] + \alpha\omega_0\frac{1}{50}\{-3c^2s^2(\lambda-1)^2(c^2+s^2\lambda)^2 - 4c^{4s4}(\lambda-1)^4 - c^2s^2(\lambda-1)^2\lambda^{-2} + 15c^2s^2(\lambda-1)^2(s^2+c^2\lambda)^2 - 2c^2s^2(\lambda-1)^2(s^2+c^2\lambda)(c^2+s^2\lambda) + (s^2+c^2\lambda)^2(c^2+s^2\lambda)^2 + (s^2+c^2\lambda)^2\lambda^{-2} + 6(s^2+c^2\lambda)^4 - 3(c^2+s^2\lambda)^4 - 3\lambda^{-4} - 2(c^2+s^2\lambda)^2\lambda^{-2}\} \quad \text{(A1)}$$

Equation A1 reduces to zero, as required, for $\lambda = 1$, and for small λ is quadratic in cos Θ.

References and Notes

(1) Deloche, B.; E. T. Samulski, *Macromolecules* **1981** *14*, 575.
(2) Deloche, B.; Beltzung. M.; Herz, J. *J. Phys. (Paris) Lett.* **1982,** *43*, 763.
(3) Gronski, W.; Stadler, R.; Jacobi, M. *Macromolecules* **1984**, *17*, 741.
(4) Toriumi, H.; Deloche, B.; Herz, J.; Samulski, E. T. *Macromolecules* **1986**, *19*, 2884.
(5) Sotta, P.; Deloche, B.; Herz, J.; Lapp, A.; Durand, D.; Rabadeaux, J.-C. *Macromolecules* **1987**, *20*, 2774.
(6) Dubault, A.; Deloche, B.; Herz, J. *Macromolecules* **1987**, *20*, 2096.
(7) Sotta, P.; Deloche, B. *Macromolecules* **1990**, *23*, 1999.
(8) McLoughlin, K.; Waldbieser, J. K.; Cohen, C.; Duncan, T. M. *Macromolecules* **1997**, *30*, 1044.
(9) Sotta, P. *Macromolecules* **1998**, *31*, 3872.
(10) Chapellier, B.; Deloche, B.; Oeser, R. *J. Phys II* **1993**, *3*, 1619.
(11) Ekanayake, P.; Menge, H.; Ries, M. E.; Brereton, M. G. *Macromolecules* **2002**, *35*, 4343.
(12) Ries, M. E.; Brereton, M. G.; Klein, P. G.; Ward, I. M.; Ekanayake, P.; Menge, H.; Schneider, H. *Macromolecules* **1999**, *32*, 4961.
(13) Kuhn, W.; Grün, F *Kolloid Z. Z. Polym.* **1942**, *101*, 248.
(14) Tjandra, N.; Bax A. *Science*, **1997**, *278* 1697.
(15) Bax, A.; Tjandra N, *J. Biomol. NMR* **1997**, *10*, 289.
(16) Tycko, R. J.; Blanco. F. J.; Ishii, Y. *J. Am. Chem. Soc.* **2000**, *122*, 9340.
(17) Ishii, Y.; Markus, M. A.; Tycko R. J, *J. Biomol. NMR* **2001**, 21, 141.
(18) Abragam, A. *The Principles of Nuclear Magnetism*; Oxford University Press: Oxford, U.K., 1961.
(19) Buckingham, A. D.; McLauchlan, K. A. *Prog. NMR Spectrosc.* **1967**, *2* 63.
(20) Arfken, G. *Mathematical Methods for Physicists*; Academic Press: New York, 1985.
(21) Luz, Z.; Poupko, R.; Samulski, E. T. *J. Chem. Phys.* **1981**, *74*, 5825.
(22) Larson, R. *Constitutive equations for Polymer Melts and Solution*; Butterworth, Stoneham, MA, 1988.
(23) Luz, Z.; Meiboom, S. *J. Chem. Phys.* **1973**, *59*, 275.
(24) Rose, M. E. *Elementary Theory of Angular Momemtum*; Wiley: New York, 1957.
(25) Saupe, A. *Z. Naturforsch.* **1964**, *A 19*, 161.
(26) Ader, A.; Loewenstein, A. *J. Am. Chem. Soc.* **1974**, *96*, 5336.
(27) Rouse, P. E. *J. Chem. Phys.* **1953**, *21*, 1272.
(28) Treloar, L. A. G. *The Physics of Rubber Elasticity*, 2nd ed.; Oxford University Press: London, 1958.
(29) Brereton, M. G. *Macromolecules* **1993**, *26*, 1152.
(30) Warner, M.; Callaghan, P. T.; Samulski, E. T. *Macromolecules* **1997**, *30*, 4733.
(31) Doi, M.; Edwards, S. F. *The Theory of Polymer Dynamics*; Clarendon: Oxford, U.K., 1986.
(32) Cormier, R. J.; Kilfoil, M. L.; Callaghan, P. T. *Phys. Rev. E.* **2001**, *64*, 1.

MA021174Z